

# Observation of Persistent Currents in Mesoscopic Connected Rings

W. Rabaud<sup>1</sup>, L. Saminadayar<sup>1</sup>, D. Mailly<sup>2</sup>, K. Hasselbach<sup>1</sup>, A. Benoît<sup>1</sup> and B. Etienne<sup>2</sup>

<sup>1</sup>Centre de Recherches sur les Très Basses Températures, B.P. 166 X, 38042 Grenoble Cedex 9, France

<sup>2</sup>Laboratoire de Microstructures et Microélectronique, B.P. 107, 92225 Bagneux Cedex, France

(October 28, 2018)

We report measurements of the low temperature magnetic response of a line of 16 GaAs/GaAlAs *connected* mesoscopic rings whose total length is much larger than  $l_\phi$ . Using an on-chip micro-SQUID technology, we have measured a periodic response, with period  $h/e$ , corresponding to persistent currents in the rings of typical amplitude  $0.40 \pm 0.08 \text{ nA}$  per ring. Direct comparison with measurements on the same rings but *isolated* is presented.

PACS numbers: 73.23.-b, 73.20.Dx, 72.20.My

In a mesoscopic metallic sample, quantum coherence of the electronic wave functions can affect drastically the equilibrium properties of the system. In the case of a metallic ring in a magnetic field, the new boundary conditions imposed by the magnetic flux [1] lead the wave functions and therefore all the thermodynamic properties of the system to be periodic with flux, with periodicity  $\Phi_0 = h/e$ , the flux quantum. One of the most striking consequences of this, first pointed out by Büttiker, Imry and Landauer [2] for the 1D case, is that a mesoscopic normal-metal ring pierced by a magnetic flux carries a persistent non-dissipative current: this is a consequence of the periodicity of the free energy  $\mathcal{F}(\Phi)$  with flux, implying the existence of an equilibrium current  $I(\Phi) = -\partial\mathcal{F}(\Phi)/\partial\Phi$ . Subsequently, much theoretical effort has been devoted to the description of a realistic 3D disordered ring [3–7]. Both the sign and the amplitude of this current depend on the number of electrons in the ring and on the microscopic disorder configuration: thus this current, like other mesoscopic phenomena such as Aharonov-Bohm conductance oscillations [8], is sample specific. However, the order of magnitude of the current for a single, isolated ring can be characterized by its typical value  $I_{typ} = \sqrt{\langle I^2 \rangle}$ ,  $\langle \rangle$  denoting the average over disorder configurations. It is given [6,7] by  $I_{typ} = 1.56 I_0 l_e / L$ . In this formula,  $I_0 = ev_F / L$  where  $v_F$  is the Fermi velocity and  $L$  the perimeter of the ring, and  $l_e$  is the elastic mean free path: the current varies as the inverse of the diffusion time  $\tau_D = L^2 / D$  where  $D = v_F l_e$  is the diffusion constant. When measuring an ensemble of rings, the typical current per ring decreases as  $1/\sqrt{N_R}$ , where  $N_R$  is the number of rings. At finite temperature [6,7,9], mixing of the energy levels reduces the current on the scale of the Thouless energy  $E_c$ , the energy scale for energy correlations. Further reduction arises when temperature reduces the phase coherence length  $l_\phi$  down to values lower than  $L$ .

For a long time, persistent currents were believed to be a specific property of isolated systems [2]. However, recent theoretical predictions suggest that persistent currents should exist even in connected rings. Using a semi-classical model in the diffusive limit, ref. [10] calculated persistent currents in various networks of connected rings, showing that the amplitude of the persistent currents should be reduced only weakly as compared to its value in the same network of isolated rings, whereas all the other properties, like temperature dependance, should be similar. The reduction factor  $r = I_{\text{connected}} / I_{\text{isolated}}$  depends on the geometry of the network. For a line of connected rings separated by arms longer than  $l_\phi$ , a simple fraction  $r = 2/3$  was predicted [10]; for the geometry considered here, it is expected [11] that  $r \approx 0.58$ . Moreover, this result is independent of the total size of the system, even much larger than  $l_\phi$ . This suggests that persistent currents could be observed in a macroscopic system. However, no experimental evidence of persistent currents in such a connected geometry has been reported up to now.

A couple of key experiments have confirmed the existence of persistent currents in isolated systems, either an ensemble of isolated rings [12–14], or a single isolated ring [15,16]. However, the amplitude of the currents found in ref. [12] and ref. [15], much larger than expected, is still not understood. In this context, the need for new experiments to clarify these results and provide new experimental facts is very important. Moreover, the existence of persistent currents in a network of connected rings larger than  $l_\phi$  remains to be experimentally demonstrated.

In this Letter, we report on measurement of the low temperature magnetic response of a line of 16 GaAs/GaAlAs *connected* rings. The experiment was performed at the base temperature of the dilution fridge in order to maximize the signal. The sample was designed so that its total size was much larger than  $l_\phi$ , while the perimeter of each ring was smaller than  $l_\phi$ . We developed a new experimental setup based on a multi-loop  $\mu$ -SQUID gradiometer, and observed a periodic response of the magnetization with period  $\Phi_0 = h/e$ , corresponding to persistent currents in the rings of amplitude  $0.40 \pm 0.08 \text{ nA}$  per ring. Using gates, we performed measurement on the same rings but *isolated*. We also observed an  $h/e$  periodic signal, corresponding to persistent currents in the rings whose amplitude is similar to the one observed for connected rings.

The GaAs/GaAlAs heterojunction was grown using molecular beam epitaxy. The structure of the epilayers is  $1\text{ }\mu\text{m}$  GaAs buffer layer,  $15\text{ nm}$  GaAlAs spacer layer,  $48\text{ nm}$  Si doped GaAlAs layer and  $5\text{ nm}$  GaAs cap layer. At  $4.2\text{ K}$  in the dark, the two dimensional electron gas (2DEG) at the heterointerface had an electron density of  $5.2 \times 10^{11}\text{ cm}^{-2}$  and a mobility of  $0.8 \times 10^6\text{ cm}^2\text{ V}^{-1}\text{ s}^{-1}$ . This yields a Fermi velocity  $v_F = 3.16 \times 10^5\text{ m s}^{-1}$  and a Fermi wavelength  $\lambda_F = 35\text{ nm}$ . All the lithographic operations were performed using electron beam lithography on PMMA (polymethyl methacrylate) resist with a JEOL 5DIIU electron beam writer. We first patterned an aluminium mask of the rings (see fig.1), which was removed after etching  $5\text{ nm}$  of the GaAs cap layer by ion milling with  $250\text{ V}$  argon ions. This was sufficient to deplete the underlying 2DEG. The rings, actually squares of internal side length  $2\text{ }\mu\text{m}$ , external side length  $4\text{ }\mu\text{m}$ , mean perimeter  $L = 12\text{ }\mu\text{m}$ , connected by  $2\text{ }\mu\text{m}$  long arms, are connected to AuGeNi ohmic contacts in a two-probe geometry. Using a similar technique we fabricated wires of different widths to characterize the sample after etching. For wires of similar width, we measured a phase coherence length  $l_\phi \approx 20\text{ }\mu\text{m}$  derived from weak localisation. Conductance measurements gave an elastic mean free path of  $l_e \approx 8\text{ }\mu\text{m}$ , and a depletion length of  $100\text{ nm}$  on each side of the wire due to the etching process. Therefore the effective width of the arms of our rings is  $W = 0.8\text{ }\mu\text{m}$ . It should be noted that in this experiment, we were not in the pure diffusive case since  $l_e \lesssim L$ , but it is expected that the analytical results for the diffusive case still apply [17]. Three Schottky gates were then deposited allowing to deplete the 2DEG underneath. The first one ("G<sub>1</sub>" in fig.1) was deposited on top of each ring and allows all the interference effects in the rings such as the persistent currents to be suppressed. The second gate ("G<sub>2</sub>") was deposited on the two outgoing wires ("Ω") and made possible the insulation of the rings from the ohmic contacts. The last one ("G<sub>3</sub>") was placed on each arm joining two rings, allowing the measurement of isolated rings. A calibration loop with the same dimensions as one ring was patterned in order to calibrate our experimental setup. Gates and calibration loop were obtained by liftoff of  $10\text{ nm}$  titanium and  $50\text{ nm}$  gold films. The device was then covered with a  $60\text{ nm}$  insulating layer (AZ 1350 resist baked at  $170^\circ\text{C}$ ).

The next step (see fig.1) was the fabrication of the μ-SQUID. It is designed as a gradiometer, equivalent to two counter-wound loops, in order to compensate the external magnetic flux [16,18], and made of aluminium because of its low critical current and the possibility to easily connect separate levels. The first level was deposited on top of the rings and of the calibration loop. Then a new insulating layer was deposited and the gradiometer was completed with the other half. The two Dayem microbridge Josephson junctions,  $300\text{ nm} \times 20\text{ nm} \times 30\text{ nm}$ , were lithographically defined at this stage. The contact be-

tween the two aluminium levels was obtained by covering them with aluminium pads deposited after an ion bombardment cleaning. The first μ-SQUID layer was made of  $60\text{ nm}$  thick aluminium and the second one, containing the two Dayem micro-bridges, of  $30\text{ nm}$  thick aluminium in order to reduce the critical current of the μ-SQUID. As the μ-SQUID has exactly the same shape as the rings, the coupling between them is almost perfect [18].

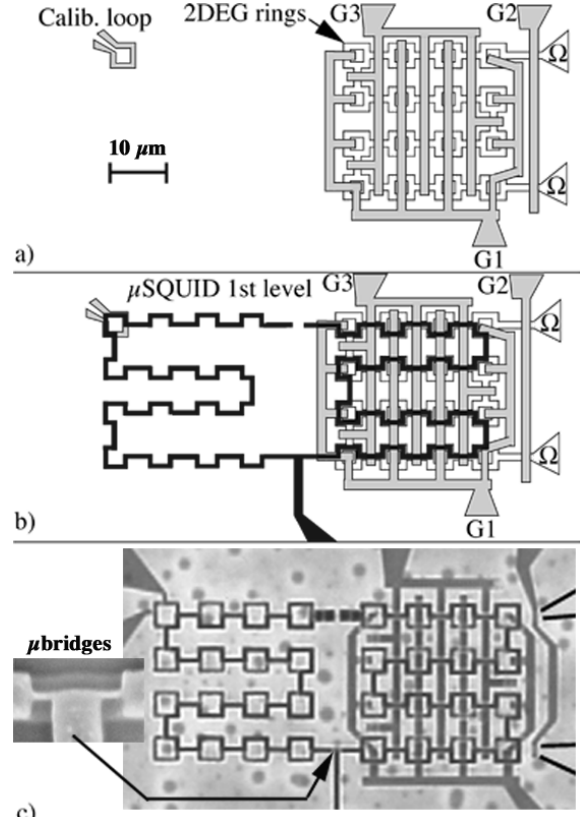


FIG. 1. Fabrication of the sample: a) Etching of the rings and the ohmic contacts ( $\Omega$ ), and deposition of the three gates ( $G_1$ ,  $G_2$  and  $G_3$ ) and the calibration loop (calib. loop). b) First level of the μ-SQUID. c) Optical photograph of the sample, including the second level of the μ-SQUID. Inset shows an SEM picture of the microbridges.

The gradiometer design and the accuracy of the e-beam lithography allow compensation of the external magnetic flux of 99.96 %. The magnetic field was swept from  $-33.5\text{ G}$  to  $-3.5\text{ G}$  at  $7.5\text{ G s}^{-1}$ , corresponding to  $3\Phi_0$  and  $9\Phi_0$  in each ring for the inside and outside trajectories respectively: in this range of magnetic field, the external magnetic flux is almost perfectly compensated, and the gain of the gradiometer, calibrated by sending a dc current through the calibration loop, nearly constant. Moreover, such a limitation in the magnetic field sweep avoids flux penetration in the Al layers of the μ-SQUID. The critical current of the μ-SQUID was measured using dedicated electronics which ramps a dc current until the μ-SQUID's critical current is attained [18]. The current is then reset, and the value of the critical current sent to a

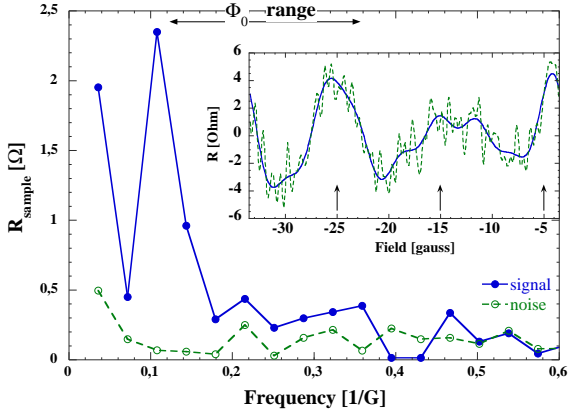


FIG. 2. Typical power spectrum of the Aharonov-Bohm conductance oscillations in a line of 16 rings, measured at  $20\text{ mK}$ . The horizontal arrow indicates the  $\Phi_0$  frequency window, calculated from the geometrical parameters of our sample. The Aharonov-Bohm peak is just one point out of this window, due to the discretization on the frequency axis. Open circles correspond to noise, i.e. FFT of the difference between two successive measurements. Solid circles correspond to signal. Increase of the signal at low frequency is due to weak localisation and universal conductance fluctuations, which are cancelled in the "noise" measurements. Inset shows the raw data after subtraction of the linear background (dashed line) and after bandpassing the signal over the  $\Phi_0$  frequency range (solid line).

computer. This cycle is repeated periodically at  $5\text{ kHz}$ , and the measured flux resolution of our gradiometer is then  $\approx 5 \times 10^{-4} \Phi_0/\sqrt{\text{Hz}}$ .

Resistance measurements as a function of magnetic field were performed separately using a conventional ac lock-in technique, with an ac current of  $100\text{ pA}$  at  $777\text{ Hz}$ . Fig.2 shows the square root of the power spectrum of the resistance measured at  $20\text{ mK}$ , obtained by Fast Fourier Transform (FFT) of the data. The horizontal scale shows the field frequency expressed in  $\text{G}^{-1}$ . Because of the aspect ratio of the rings, the  $\Phi_0$  frequency extends from  $0.12\text{ G}^{-1}$  to  $0.35\text{ G}^{-1}$ . The spectrum clearly exhibits a peak in the  $\Phi_0$  frequency range, corresponding to Aharonov-Bohm conductance oscillations. The separation between each point of the FFT is directly related to the range of magnetic field used, which leads to a discretization of  $0.036\text{ G}^{-1}$  on the frequency axis.

To measure the persistent currents, the critical current of the  $\mu$ -SQUID was measured as a function of the magnetic field. We performed measurements with the rings "opened" and "closed" ( $-561\text{ mV}$  applied on the gate  $G_1$  when measuring opened rings). The rings were insulated from the ohmic contacts by applying  $-558\text{ mV}$  on the gate  $G_2$ . Each measurement represented about  $1\text{ min}$  of accumulation time. The signal of persistent currents was then extracted by FFT of the difference between measurements with closed and opened rings, whereas the noise was obtained by FFT of the difference between two

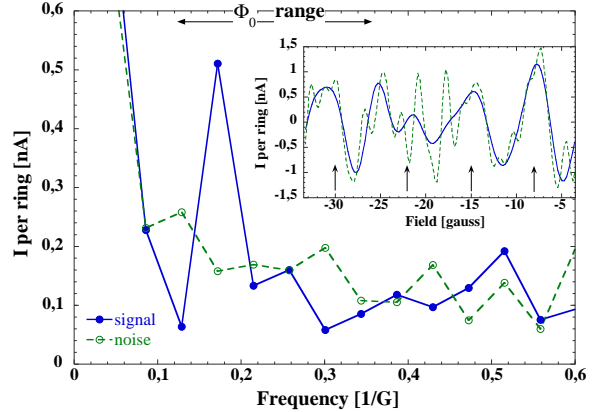


FIG. 3. Typical power spectrum of the magnetization due to persistent currents in a line of 16 connected rings expressed in  $\text{nA}$  per ring, measured at  $20\text{ mK}$ . The horizontal arrow indicates the  $\Phi_0$  frequency window, calculated from the geometrical parameters of our sample. Open circles correspond to noise, i.e. FFT of the difference between two identical measurements. Solid circles correspond to signal, i.e. FFT of the difference between measurements with the rings closed and opened. Inset shows the raw data after subtraction of the linear background (dashed line) and after bandpassing the signal over the  $\Phi_0$  frequency range (solid line).

identical measurements, either closed or opened rings. Thus one spectrum (see fig.3) was obtained in about  $4\text{ min}$ . This possibility of background noise subtraction is an important advantage of our experimental technique [16]. The total signal was divided by 16 to obtain the current per ring.

A typical result for the square root of the power spectrum of the persistent currents expressed in  $\text{nA}$  per ring is depicted in fig.3. The increase of the signal at low frequency is mostly due to slow temporal fluctuations of the critical current of the  $\mu$ -SQUID. Note that contrary to previous experiments [16], the aspect ratio of the rings allows the signal to extend over several units of the FFT abscissa, corresponding to the  $\Phi_0$  frequency range [8]: the amplitude of the persistent currents is then obtained by taking the difference between the area under the  $\Phi_0$  region of the "signal" and the "noise" curves. By this means, the fact that we do not observe any increase of the amplitude of the "noise" curve in the  $\Phi_0$  frequency range of fig.3 but an increase of the amplitude of the "signal" curve is a clear signature of persistent currents in our line of connected rings.

It should be stressed that random modifications of the disorder configuration of the sample occurred due to relaxation processes of the dopants in the GaAlAs layer; this explains why the signal varied in amplitude on a time scale of  $\approx 15\text{ min}$ . It is this instability that allows us to perform statistics over the amplitudes of the persistent currents corresponding to different disorder configurations, and thus to measure the typical current [16]. Using this technique over a sample of  $\approx 1000$  spectra, we

find for our line of 16 connected rings after subtraction of the noise, a typical current of  $0.40 \pm 0.08 \text{ nA}$  per ring. This value has to be compared with the theoretical value  $0.58 \times 1.56 (I_0/\sqrt{N_R}) (l_e/L) \approx 0.63 \text{ nA}$  per ring,  $r = 0.58$  being the reduction factor predicted for the same line of connected rings and  $I_0$  being derived from our experimental parameters.

By applying  $-540 \text{ mV}$  on the gate  $G_3$  we isolated the rings and performed the same experiment as for connected rings. We also observed an  $h/e$  periodic signal, corresponding to persistent currents in the rings of  $0.35 \pm 0.07 \text{ nA}$  per ring, to be compared with the theoretical value  $1.56 (I_0/\sqrt{N_R}) (l_e/L) \approx 1.09 \text{ nA}$  per ring. Such a difference between experimental and theoretical values may be due to the finite value of  $l_\phi$  [7] as well as the exact shape of the sample (squares instead of rings).

The key point is the direct experimental comparison between persistent currents in the same rings either connected or isolated. Our experiment gave a ratio  $I_{\text{connected}}/I_{\text{isolated}} \approx 1.2 \pm 0.5$ . A similar experiment on a line of 4 rings gave a similar result. The theoretical value calculated by ref. [10,11] for the diffusive case is  $r \approx 0.58$ : the difference may be due to the fact that the model used is valid in the diffusive regime. In our samples  $l_e \lesssim L$ , and deviations from the pure diffusive case may be expected [11]. But such a ratio of order unity points out the most striking result of our experiment: *persistent currents were not significantly modified when connecting or isolating the rings*. All previous experiments were carried out on isolated rings [12–16]. Our result shows that persistent currents are not a specific property of isolated systems: in our line of rings, electrons can visit the whole sample and lose their phase coherence. However, we have shown quantitatively that the trajectories encircling individual loops, and thus giving rise to the persistent currents, are very weakly affected by the connection to arms. This result should remain valid for any two dimensional array of rings (or holes) whose perimeter is smaller than  $l_\phi$  [10]. By extension, this suggests that persistent currents could be observed in a macroscopic sample: all the closed trajectories smaller than  $l_\phi$ , which enclose flux, should give rise to a measurable persistent current, even if the whole sample is clearly not a quantum coherent object.

In conclusion, using a multiloop  $\mu$ -SQUID gradiometer, we have measured the magnetization of a line of connected GaAs/GaAlAs rings as a function of magnetic field. We have observed a periodic response, with period  $h/e$ ; the amplitude of the corresponding persistent currents is in good agreement with theoretical estimates. Measurements on the same but isolated rings also showed an oscillatory component of the magnetization with period  $h/e$ : the amplitude of the persistent currents in connected and isolated rings was found to be similar.

Further measurements on various geometries are now needed to fully understand the effect of the connectivity

of the sample on the persistent currents. Experiments in the pure diffusive case or on a larger number of rings should also help to give a correct description of this "extensive" nature of persistent currents. From the theoretical side, a model for the ballistic case is needed for a direct comparison with our experiment.

Fruitful discussions with G. Montambaux, M. Pascaud, H. Bouchiat, V. Chandrasekhar and P. Butaud are acknowledged. We thank J. L. Bret, G. Simiand, J. F. Pini and H. Rodenas for technical help, D. K. Maude and J. Gilchrist for careful reading of the manuscript.

- 
- [1] N. Byers and C. N. Yang, Phys. Rev. Lett. **7**, 46 (1961).
  - [2] M. Büttiker, Y. Imry and R. Landauer, Phys. Lett. **96A**, 365 (1983).
  - [3] H. Bouchiat and G. Montambaux, J. Phys. France **50**, 2695 (1989); G. Montambaux, J. Phys. I France **6**, 1 (1996).
  - [4] V. Ambegaokar and U. Eckern, Phys. Rev. Lett. **65**, 381 (1990).
  - [5] B. Altshuler, Y. Gefen and Y. Imry, Phys. Rev. Lett. **66**, 88 (1991); F. von Oppen and E. K. Riedel, Phys. Rev. Lett. **66**, 84 (1991); A. Schmid, Phys. Rev. Lett. **66**, 80 (1991).
  - [6] H. F. Cheung, E. K. Riedel and Y. Gefen, Phys. Rev. Lett. **62**, 587 (1989); N. Argaman, Y. Imry and U. Smilansky, Phys. Rev. B **47**, 4440 (1993); E. K. Riedel and F. von Oppen, Phys. Rev. B **47**, 15449 (1993).
  - [7] G. Montambaux, in *Quantum Fluctuations*, S. Reynaud, E. Giacobino and J. Zinn-Justin eds., Amsterdam (1997) and references therein.
  - [8] S. A. Washburn and R. A. Webb, Adv. Phys. **35**, 375 (1986).
  - [9] R. Landauer and M. Büttiker, Phys. Rev. Lett. **54**, 2049 (1985).
  - [10] M. Pascaud and G. Montambaux, Europhys. Lett. **37**, 347 (1997); Phys. Rev. Lett. **82**, 4512 (1999).
  - [11] G. Montambaux, private communication.
  - [12] L. P. Lévy, G. Dolan, J. Dunsmuir and H. Bouchiat, Phys. Rev. Lett. **64**, 2074 (1990); L. P. Lévy, D. H. Reich, L. Pfeiffer and K. West, Physica B **189**, 204 (1993).
  - [13] B. Reulet, M. Ramin, H. Bouchiat and D. Mailly, Phys. Rev. Lett. **75**, 124 (1995); Y. Noat, H. Bouchiat, B. Reulet and D. Mailly, Phys. Rev. Lett. **80**, 4955 (1998).
  - [14] P. Mohanty, Ann. Phys. (Leipzig) **8**, 549 (1999).
  - [15] V. Chandrasekhar, R. A. Webb, M. J. Brady, M. B. Ketchen, W. J. Gallagher and A. Kleinsasser, Phys. Rev. Lett. **67**, 3578 (1991).
  - [16] D. Mailly, C. Chapelier and A. Benoît, Phys. Rev. Lett. **70**, 2020 (1993).
  - [17] G. Montambaux, H. Bouchiat, D. Sigit and R. Friesner, Phys. Rev. B **42**, 7647 (1990).
  - [18] K. Hasselbach, C. Veauvy and D. Mailly, Physica C **332**, 140 (2000).